Monitoring of Local Earthquakes in Haiti Using Low-Cost, Citizen-Hosted Seismometers and Regional Broadband Stations

Sylvert Paul[*1,2,3], Tony Monfret[2,3,4], Françoise Courboulex[2,3], Jérôme Chèze[2,3], Eric Calais[2,3,5], Steeve Julien Symithe[1,3], Anne Deschamps[2,3], Fabrice Peix[2,3], David Ambrois[2,3], Xavier Martin[2], Sadrac St Fleur[1,3], and Dominique Boisson[1,3]

Abstract

Seismic monitoring in Haiti is currently provided by a mixed network of low-cost Raspberry Shake (RS) seismic stations hosted by citizens, and short-period and broadband stations located mainly in neighboring countries. The level of earthquake detection is constantly improving for a better spatio-temporal distribution of seismicity as the number of RS increases. In this article, we analyze the impact of the quality of the signals recorded by the RS—low-cost seismometers with the smallest magnitude that the network can detect by studying the ambient noise level at these stations. Because the RS stations are installed as part of a citizen-science project, their ambient noise estimated by the power spectral density (PSD) method often shows a high-noise level at frequencies above 1 Hz. In the near field (< 50 km), we show that the network detects seismic events of local magnitude on the order of 2.2 with signal-to-noise ratios (SNRs) greater than 4. Improving the network detection threshold requires densifying the network with more RS stations in locations that are less noisy, if possible. In spite of these limitations, this mixed network has provided near-field data essential to rapidly understand the mechanism of the mainshock of the 14 August 2021 M_w 7.2 earthquake, to monitor its sequence of aftershocks in near-real time, and to monitor background seismicity in Haiti on a routine basis.

Cite this article as Paul, S., T. Monfret, F. Courboulex, J. Chèze, E. Calais, S. Julien Symithe, A. Deschamps, F. Peix, D. Ambrois, X. Martin, *et al.* (2023). Monitoring of Local Earthquakes in Haiti Using Low-Cost, Citizen-Hosted Seismometers and Regional Broadband Stations, *Seismol. Res. Lett.* **XX**, 1–15, doi: 10.1785/0220230059.

Supplemental Material

Introduction

The island of Hispaniola straddles the boundary between the Caribbean and North American plates, which are converging obliquely at 19 mm/yr (DeMets *et al.*, 2000). This relative plate motion is partitioned between left-lateral strike-slip on the Septentrional and Enriquillo faults at 10 and 7–8 mm/yr, respectively, and reverse motion on the north Hispaniola fault at 3–4 mm/yr (Manaker *et al.*, 2008; Symithe *et al.*, 2015). The island has experienced a number of destructive earthquakes in the historical period (Fig. 1), first cataloged by Scherer (1912) and more recently reinterpreted by Bakun *et al.* (2012). The earliest historical event reported occurred on 2 December 1562 in the northern part of the Dominican Republic, destroying the first city of the so-called "New World"—Santiago de Los Caballeros (Utrera, 1927). In Haiti, the first earthquake mentioned in the historical catalog occurred on 9 November 1701, with an epicenter located near the city of Léogâne and a magnitude estimated at 6.6 (Bakun *et al.*, 2012). It was followed by four other destructive events in the southern part of the island, likely striking the Enriquillo fault system, on the 18 October 1751 **M** 7.5, 21 November 1751 **M** 6.6, 3 June 1770 **M** 7.5, and 8 April 1860 **M** 6.3 earthquakes (Bakun *et al.*, 2012, Hough *et al.*, 2023; Martin and Hough, 2022). In northern Haiti, the Septentrional fault was likely the locus of the 7 May 1842 **M** 7.6 earthquake (ten Brink *et al.*, 2011) that was accompanied by a tsunami (Gailler *et al.*, 2015). It was followed on 23 September 1887 by a moderate-size event

1. Université d'Etat d'Haïti, Faculté des Sciences, URGéo, Haïti, https://orcid.org/0000-0003-4132-7635 (SP); https://orcid.org/0000-0003-1133-202X (SJS); https://orcid.org/0000-0002-7136-7235 (DB); 2. Université Côte d'Azur, CNRS, IRD, Observatoire de la Côte d'Azur, Géoazur, France, https://orcid.org/0000-0002-4521-0357 (TM); https://orcid.org/0000-0002-4467-9102 (FC); https://orcid.org/0000-0002-5935-8117 (EC); https://orcid.org/0000-0002-6209-9814 (AD); https://orcid.org/0000-0001-5384-6868 (XM); 3. CARIBACT Joint Research Laboratory, IRD/UCA/UEH, Port-au-Prince, Haiti; 4. Barcelona Center for Subsurface Imaging, Institut de Ciències del Mar (ICM), CSIC, Barcelona, Spain; 5. École Normale Supérieure, Université PSL, Paris, France

*Corresponding author: sylvert.paul@geoazur.unice.fr

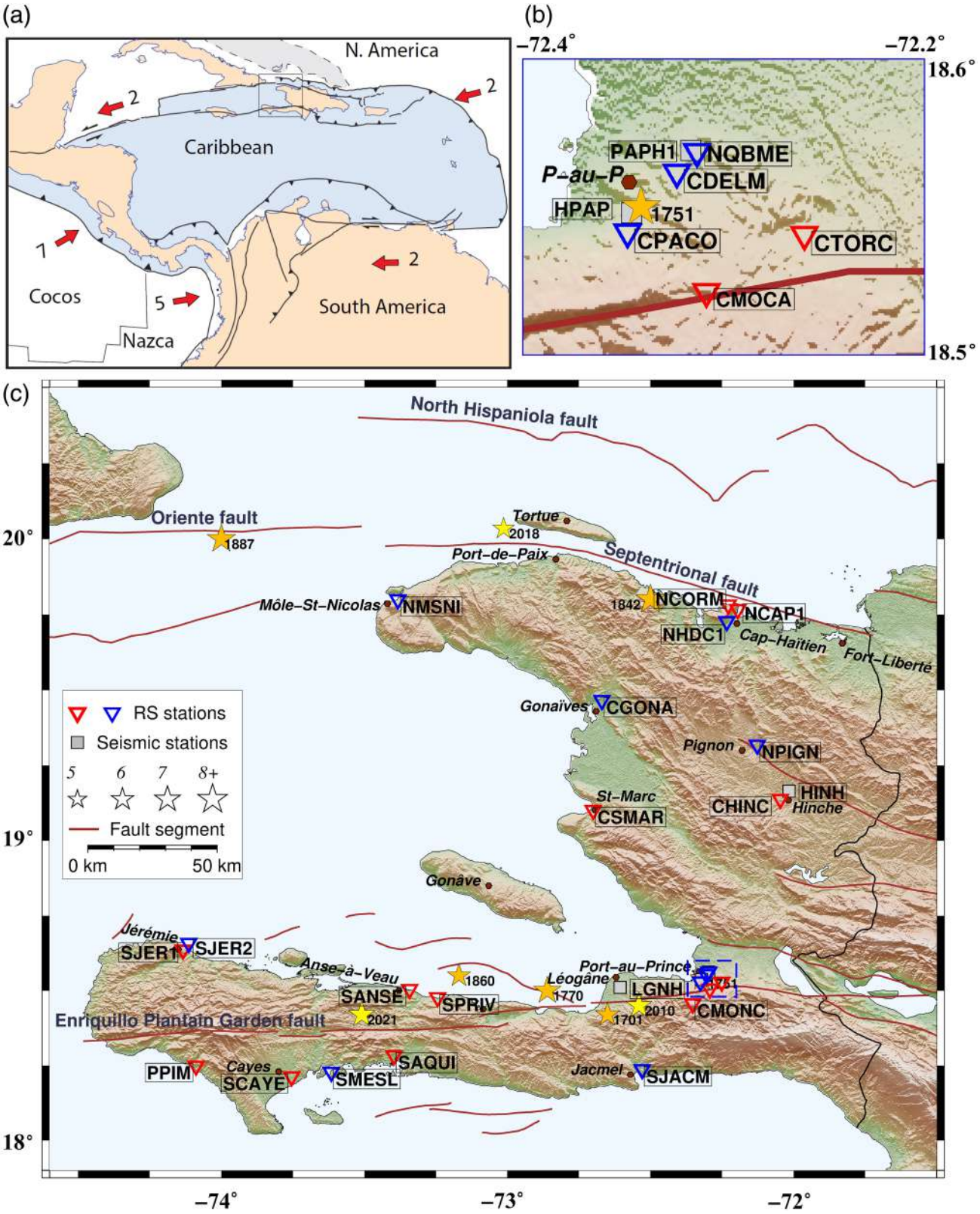

Figure 1. Historical seismicity of Haiti and location of the seismic stations used in this study. (a) Seismotectonic context of the Caribbean—North American plate boundary. The black solid rectangle displays the area shown in panel (c), and the red arrows show the relative motion of plates to the Caribbean plate (cm/yr). (b) Zoom-on the RS stations located in the Port-au-Prince area (blue dashed line box in panel c). (c) Main active fault systems are shown with brown lines. The stars indicate historical (orange) and instrumental (yellow) earthquakes (McCann, 2006; Bakun *et al.*, 2012; Calais *et al.*, 2022). The inverted open triangles are Raspberry Shake (RS) stations of the HY network. Those with blue color are used in this study. Other stations installed in Haiti are not used in this study (gray squares). The color version of this figure is available only in the electronic edition.

M 6.7 located between Cuba and Haiti (ten Brink *et al.*, 2011), likely striking the Septentrional fault as well.

In spite of this well-established historical record, little attention was paid to active tectonics in Haiti until the catastrophic earthquake of 12 January 2010, except for regional geological mapping of active faults (Mann *et al.*, 1995) and early Global Positioning System (GPS) measurements of fault-slip rates (Manaker *et al.*, 2008). As a result, no seismic monitoring network was in place when that earthquake struck, except for a short-period educational seismometer located in a high school in Port-au-Prince, which saturated during the mainshock and stopped operating within minutes as the power system went down. The 12 January 2010 M_w 7.0 earthquake, with up to 230,000 death and an economic cost close to 10 billion U.S., served as a wake-up call for seismic instrumentation in Haiti, and triggered a renewal of research on active tectonics and earthquake hazard (Calais *et al.*, 2020). The earthquake ruptured an unmapped fault, secondary to the main Enriquillo plate boundary fault, with a mechanism that combined 62% of strike slip with 38% of reverse moment release (Calais *et al.*, 2010; Hayes *et al.*, 2010), similar to the 14 August 2021 M_w 7.2 event farther west on that same fault system (Calais *et al.*, 2022).

About a month after the 2010 earthquake, the Geological Survey of Canada (GSC) installed three broadband seismic stations in Port-au-Prince (PAPH, now relocated and renamed PAPH1), Léogâne, and Jacmel, with real-time satellite transmission capabilities (Bent *et al.*, 2018). This was followed by the creation of the Unité Technique de Sismologie (UTS) within the Bureau of Mines and Energy, the Haiti National Geological Survey. The UTS then installed two similar sets of instruments in Hinche (HINH) and Cap Haitien (CAPH) in the framework of a collaboration with the Seismological and Volcanological Observatory of Martinique, which included the training of Haitian technicians and the setup of a monitoring system based on SeisComP (Helmholtz-Centre Potsdam-GeoForschungsZentrum [GFZ] German Research Centre for Geosciences and Global Earthquake Monitoring Processing Analysis [GEMPA] GmbH, 2008). However, the maintenance of the instruments has proven difficult because governmental resources to UTS are scarce. As a result, the next destructive earthquake on 7 October 2018 M_w 5.9 in the northwestern part of the country, with 17 deaths, 421 injured, and 42 buildings heavily to slightly damaged, was not recorded by the national network, because its stations were not operational.

The idea then came that the expensive and hard to maintain broadband seismic stations of the Haiti National Seismic Network could be complemented by low-cost sensors that are easy to maintain, require no seismological expertise, and hence can be installed in the homes of volunteer citizens. Indeed, the major disaster of 2010 highlighted both (1) a lack of a data on the regional seismicity to produce hazard maps with a sufficient level of confidence (Frankel *et al.*, 2011); and (2) a lack of adequate communication of the seismic risk to the public, because earthquake preparedness initiatives from the government have not yet been established. Therefore, in 2019 we initiated a participatory seismology experiment in Haiti to test whether public or community involvement through the production and usage of seismic information could improve earthquake awareness and, perhaps, induce grassroots protection initiatives (Calais *et al.*, 2020). This experiment involves seismologists and sociologists in a common endeavor, with the aim of determining the potential of citizen seismology to engage the public while collecting scientifically relevant seismological information in a development context. In this article, we restrict ourselves to describing the seismological component of this project made possible, thanks to the relatively recent launch of very low-cost, plug-and-play, Raspberry Shake (RS) seismological stations (Anthony *et al.*, 2019), the relative ease of access to the internet even in developing countries such as Haiti, and the familiarity of all with social networks as a way to disseminate information.

Indeed, in spite of their limited frequency band-pass (short-period sensor), RS instruments are not only used by interested individuals but also, more and more, by academic seismologists. Anthony *et al.* (2019) first showed that, despite their relatively high-intrinsic self-noise level, RS can be used to densify conventional seismic monitoring networks for studies of local or regional seismicity. RS sensors have been used for monitoring rockfall activity (Manconi *et al.*, 2018), estimating the resonant frequency of unstable boulders (Taruselli *et al.*, 2019), and monitoring icequakes in eastern Antarctica (Winter *et al.*, 2021). They have been shown to provide a suitable alternative to conventional instruments for seismic hazard assessment (Holmgren and Werner, 2021). RS have been used to complement broadband sensors for monitoring the reduction in global ambient noise following restrictions imposed to contain the propagation Covid-19 (Lecocq *et al.*, 2020). Others are exploring their potential use for studying animal behavior (Lamb *et al.*, 2021). Moreover, the ease-of-use and connectivity of RS make them ideal instruments for promoting seismic risk awareness through proactive citizen involvement, touching on educational and social aspects (Calais *et al.*, 2020; Diaz *et al.*, 2020; Jeddi *et al.*, 2020; Subedi *et al.*, 2020).

Here, we describe the so-called "Ayiti-Séismes system," which was developed for the rapid location and magnitude estimation of regional earthquakes in Haiti based on a mix of RS stations and conventional regional broadband stations. The broadband stations include those operated by the Haiti national seismic network (Bent *et al.*, 2018). The RS instruments are hosted by volunteer citizens, usually in their homes. Contrary to conventional broadband instruments, we do not place strong constraints on the location of the RS instruments so as not to burden their hosts, who are an essential component of our "socio-seismology" experiment (Calais *et al.*, 2020; Fallou *et al.*, 2022). As a result, the noise level of the RS

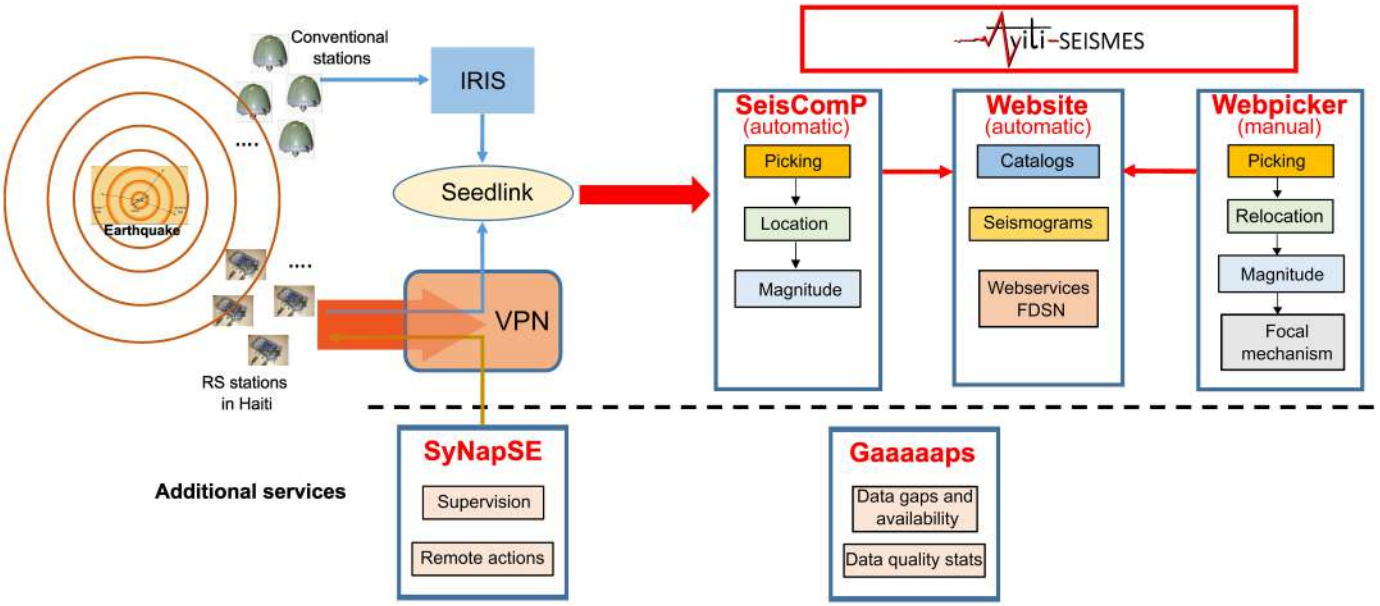

Figure 2. Schematic flowchart of the Ayiti-Séismes system from the earthquake, its recording by RS and conventional seismic stations, the data flow, the detection and location and magnitude estimation, and the posting of the results at the web portal. The additional services SyNApSE and Gaaaaaps are the tools available to the maintenance staff to follow station operation and data quality. The color version of this figure is available only in the electronic edition.

instruments is highly variable, as will be described subsequently. In spite of the limitation of the RS data in terms of instrumental response and site quality, they provided essential real-time information following the 14 August 2021 M_w 7.2 earthquake (Calais *et al.*, 2022), showing that the Ayiti-Séismes system as a whole allows one to monitor large events and their aftershock sequence. Here, we analyze the noise level of 10 of RS instruments, and show a few examples of earthquake locations performed by the system.

The Ayiti-Séismes System

Overview

The Ayiti-Séismes system relies on the automatic processing of real-time data flows retrieved from several types of seismological stations with various transmission modes (a schematic view of the system is provided in Fig. 2). In addition to data from classical broadband stations accessible through the Institutions of Research in Seismology (IRIS) public SeedLink server, the Ayiti-Séismes system makes use of a network of RS sensors, which has been progressively developing in Haiti, now under the International Federation of Digital Seismograph Networks (FDSN) code "HY" (Université d'Etat d'Haïti, 2019).

The HY network is composed of three types of stations: (1) RS1Ds, with a single vertical geophone of cutoff frequency at 4.5 Hz, electronically extended to 0.5 Hz; (2) RS4Ds with a single vertical geophone and an integrated 3D micro-electromechanical system accelerometer that enables the recording of strong motions without saturation under large shaking; and (3) RS3Ds with three-component geophones with the same technical characteristics than for RS1D instrument. Each RS contains a built-in digitizer and transmits data in miniSEED format in real-time via SeedLink protocol; its sampling rate is 100 samples/s, and its timing accuracy is controlled by network timing protocol. The diversity of sensors and acquisition units is compensated for by the introduction into the processing chain of metadata in stationXML1.1 format, freely provided by IRIS or produced with METEOR tools (Chèze *et al.*, 2020), developed within the framework of the French seismological and geodetic network (RESIF) project (re3data.org, 2022). METEOR is an online tool that allows a user to fill in all the required information of a station to produce its instrumental response in a standard format (FDSN StationXML). The RS stations in Haiti are hosted by citizens who freely provide the electric power necessary for the instrument to operate and share their Internet connection to transmit the data (for examples of installation Fig. S1, available in the supplemental material to this article). The technical challenge then was to establish the connection between the detection system and the RS that is connected on the internal private network of the host without interfering with the host's network equipment. The solution to this problem is the implementation of a virtual private network (VPN) that connects the RS to the detection system (Fig. 2). Each RS is configured with its own VPN key. When Internet access is available, the RS connects to the VPN server, which allows the detection system to retrieve the data in real time via SeedLink. This VPN connection also allows one to retrieve, at regular intervals, the health status of the stations to ensure their supervision with the National

System for Equipment Supervision (SyNApSE, 2021) tool. In parallel, the Gaaaaaps tool (see Data and Resources) allows for a visualization of the availability of archived data and displays statistical values of raw signal such as root mean square, standard deviation, and mean value that provides information on the quality of the data. The real-time data streams are openly available from Ayiti-Séismes system website using FDSN protocols.

The automatic detection of events is ensured by the SeisComP software (Helmholtz-Centre Potsdam-GFZ German Research Centre For Geosciences and GEMPA GmbH, 2008), which allows for the real-time processing of received data, the detection of events, and the automatic calculation of their location and magnitude. We impose the minimum number of four stations not only to compute a first location and magnitude, but also to minimize false detections. This number may evolve when the number of available stations will increase. The events are then reviewed by seismologists who validate and refine the results using the WebPicker tool (see Data and Resources). This tool allows for the post-processing of the events by manual picking of the arrival times, hypocenter re-estimation, and magnitude calculation. Focal mechanisms can also be determined manually if sufficient reliable *P* polarities are available. WebPicker does not require the installation of a platform-dependent application, and allows users to remotely and collectively work on any event detected to confirm and/or improve its location or magnitude. It proved very efficient in the wake of the 14 August 2021 M_w 7.2 earthquake, because it made it possible to set up in a very reactive way a team of 10 people working simultaneously to process its numerous aftershocks (Calais *et al.*, 2022).

Both locations and magnitudes are evaluated with the standard SeisComP modules. We use the scmag module to calculate the magnitude M_L (amplitudes measured on the vertical component) for all the RS and LOCSAT locator with IASPEI91 velocity model for event location.

All the information derived from this analysis, including automatic arrival times, is available in an open-access database through a web application accessible remotely using any internet browser. We currently restrict access to the manually reviewed arrival times to users with authentication information, which can be obtained upon request (see Data and Resources). The location and magnitude results are available in quasi-real-time at the Ayiti-Séismes system website. Automatic results are typically available within 120–180 s after the event, whereas the timeliness of manual reviews depends on the availability of the operators, but is typically on the order of 180 s–48 hr. The home page of the website displays a map of the recent earthquakes (last 7 days) with a square symbol for the automatic locations and a circle symbol for manually reviewed ones. The earthquake time at the website uses local time in Haiti, to be understood by everybody there. The website includes a number of additional functionalities. For instance, one can search the catalog of the recorded events for a given interval of time, plot the time distribution of the seismicity, the frequency-magnitude distribution of the catalog, or the list of stations that recorded a particular event. One can also choose to select all the earthquakes recorded by a specific RS (or other) station, which is a way to incentivize RS hosts, because they can directly observe the impact of their station on the overall catalog.

Earthquake location

Because the system became operational, 4104 earthquakes were located from August 2019, until June 2022 (Figs. 3 and 4). Before the 14 August 2021 M_w 7.2 Nippes earthquake (yellow star in Fig. 3), most of the events had magnitudes between 2 and 4, with some rare peaks not exceeding magnitude 5, and do not exceed 30 events per month on an average (Fig. 4). Some rare events with very small magnitudes could also be located, the smallest of them with a magnitude of 0.5. The number of events increased very sharply after the 2021 Nippes earthquake to 120 per day on an average during the first few weeks of the aftershock sequence and remained at 10 per day on an average as of June 2022 (Fig. 4).

Figure 5 shows the frequency–magnitude distribution and *b*-value analysis for earthquakes recorded by the Ayiti-Séismes system before and after the mainshock of 14 August 2021. The application of the Gutenberg–Richter law to the catalog gives a *b*-value of 0.982 ± 0.083 estimated from the maximum likelihood method (Aki, 1965) and a magnitude of completeness (M_c) of 2.4 before the Nippes event (Fig. 5a). It is similar to the global average *b*-value of 1 for the global Earth. The postseismic activity following the event of 14 August 2021 dominates the second part of the catalog and gives a *b*-value of 0.903 ± 0.041 with an M_c of 2.5 (Fig. 5b). After such a large event, we expected an increase in *b*-value due to local stress changes in the aftershock area (Gulia *et al.*, 2018). We observed that the SeisComP system did not have the technical capacity to detect, in real time, earthquakes that occurred less than one minute after the detection of an event. This technical bias can be corrected by analyzing the seismic sequences in delayed time, either manually or by means of more efficiency detectors such as artificial intelligence-based or matched-filter techniques (Shelly *et al.*, 2007; Zhu and Beroza, 2019; Zhou *et al.*, 2022). Currently, Ayiti-Séismes does not have such a system in operation for real-time detection and location. Therefore, during the first days of the Nippes seismic crisis, Ayiti-Séismes was not able to detect and locate all aftershocks of magnitude >2.4, which would have led to an M_c higher and a *b*-value lower than expected. Between 2013 and 2014 and using a 1 yr temporary seismic network deployed along a north–south transect across Haiti, Possee *et al.* (2019) obtained a *b*-value of 1.07 (±0.09), which was still influenced by aftershocks of the 12 January 2010 M_w 7.0 earthquake. In neighboring countries, Moreno Toiran (2002) found a *b*-value of 0.95 for southeast Cuba, Wiggins-Grandison (2001) found a

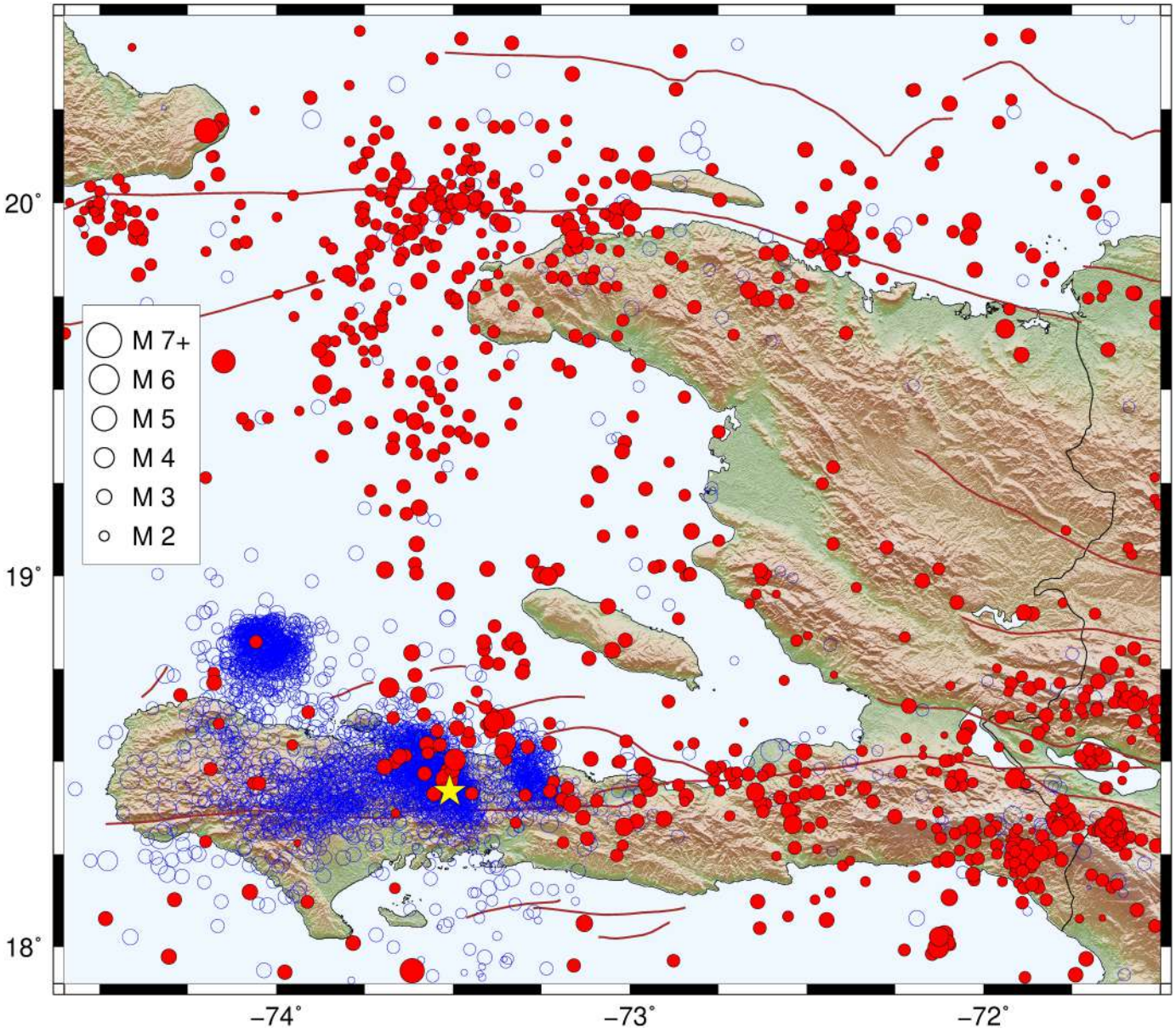

Figure 3. Map of the seismicity catalog of the Ayiti-Séismes system. The red circles show events recorded from its start in August 2019 to 13 August 2021. Empty blue circles show events recorded from the mainshock of 14 August 2021 M_w 7.2 (yellow star, epicenter from Calais *et al.*, 2022) to 30 June 2022. The color version of this figure is available only in the electronic edition.

b-value of 1.02 for Jamaica, and Johnson *et al.* (2021) found a *b*-value of 1.06 in the Dominican Republic.

Noise Analysis

Most of the RS stations are installed in cities, with little effort to minimize or mitigate anthropogenic noise (Calais *et al.*, 2020). Given this RS deployment strategy, it is important to quantify the noise level of the instruments to document their performance range, which varies significantly among stations and as a function of time.

Data availability

RS stations were installed progressively over time, starting in January 2019. The Ayiti-Séismes system then became operational from August 2019 (for a complete distribution of available data from installation to see Fig. S2). We analyzed continuous waveform segments at each RS station from their installation date onward. The availability of continuous RS data is highly dependent on the ability of the hosts to supply electricity and an internet connection, because the national electricity company (Electricité d'Haïti [EDH]) does not provide continuous power. One must then complement the few hours per day of EDH power with diesel generators and/or solar panels attached to the batteries and an inverter, a privately owned system, continuity for which depends on the

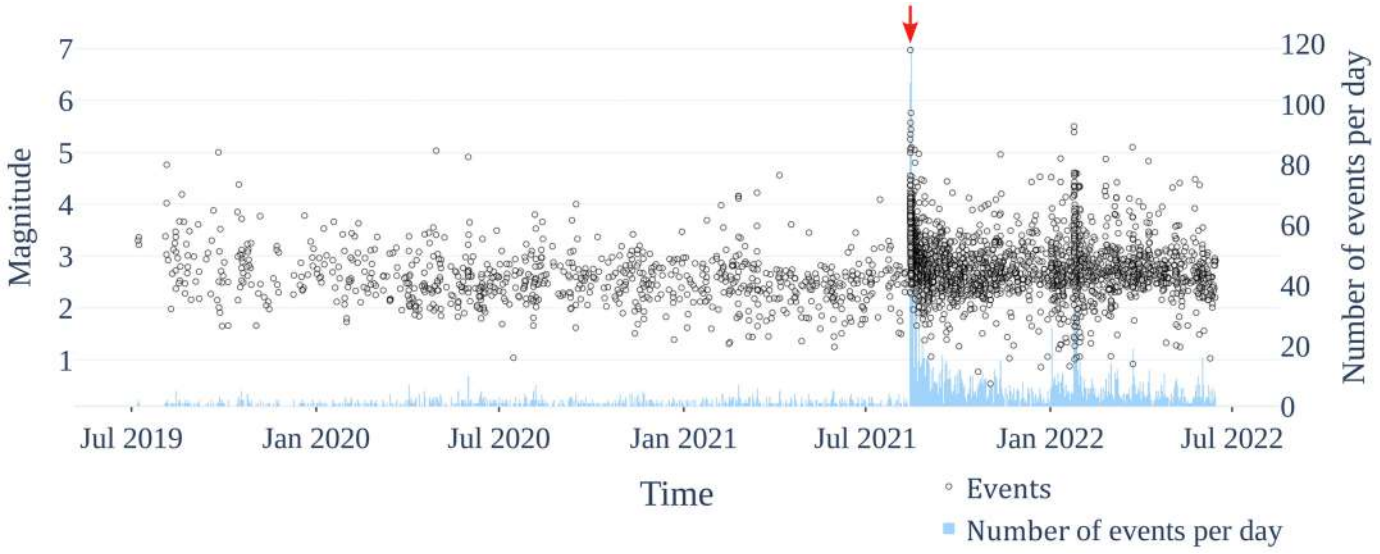

Figure 4. Temporal seismicity distribution of the Ayiti-Séismes catalog from August 2019 to 30 June 2022, black circles show event magnitudes (M_L), and blue bars show number of events per day. 4104 earthquakes are listed. The number of earthquakes detected per day reached 120 after the M_w 7.2 earthquake of 14 August 2021 (red arrow) and remains around 10 per day on June 2022. The color version of this figure is available only in the electronic edition.

hosts' motivation and welfare. This drawback, anticipated from the project outset, is mitigated by the fact that the low cost of RS stations permits the installation of several instruments in the same city or vicinity, ensuring a form of "maintenance" of the network through spatial redundancy. For instance, three stations installed in the city of Jérémie or in the city of Cap Haitian (Fig. 1) complement each other when the data stream of one of them becomes unavailable.

We selected RS datasets having 73.3%–99.9% of continuous data available over a time window between January and March 2020 or 2021 (Table 1) to ensure a good statistical evaluation of the noise level. We chose this time period because it corresponds to the dry season in Haiti without storms. Therefore, the data intervals selected are not always contemporaneous across RS instruments. Discontinuities (RS data availability <100%) observed in the recordings are often due to interruptions in the power supply and/or Internet connection, or defective micro-SD cards. Less often, we observed problems with the SD card of the RS instrument, which could generally be recovered by a reboot of the RS, imposing a daily control of all the RS. In case of transmission failure due to Internet problems, the recovery of the missing data still in memory is done automatically once the network connection is restored. In other cases, it results in gaps in the datasets. This explains the disparity between the availability of RS station data since its beginning, which varies from 41.9% to 93.1% (Fig. S2).

Method

To determine the ambient-noise intensity at each site, we calculate the power spectral density (PSD) of the noise in the frequency band between 0.05 and 30 Hz using the Obspy software (Beyreuther *et al.*, 2010). We use the manufacturer's instrumental specifications to remove the instrument response. The detailed evaluation of the performance of RS stations by Anthony *et al.* (2019) shows that the error in amplitude is less than 5%, as the geophone dynamic range is 130 dB (~21.5 bits of resolution) at 1 Hz. We only used the velocimetric vertical component of the RS stations, because their self-noise level is significantly below that of the accelerometer component.

We follow the methodology proposed by McNamara and Buland (2004), in which the waveforms are divided into 50% overlapping 1 hr long segments to reduce the variance in the PSD estimation. Within each frequency band (octave), the calculated average PSD is stored along with the value of the octave center frequency. To further reduce the variance of the final PSD estimates, the 1 hr file is further divided into 13, 75% overlapping time-series segments. Then, each of these segments is truncated to the next lower power of 2, and its Fast Fourier Transform is calculated (Cooley and Tukey, 1965). During spectral processing, low-frequency linear trends are removed by the mean slope method to avoid large distortions. To minimize aliasing effects due to truncated and detrended time series, a 10% cosine taper is applied to the ends of each segment. This is taken into account in the estimation of the PSD by a correction factor of 1.142857 (McNamara and Buland, 2004). Thus, to ensure that the PSD is sufficiently smooth, for each continuous waveform segment, it is estimated at each 1/8 of an octave, and the powers obtained are accumulated in 1 dB bands. Statistical analysis of the PSD curves allows for the generation of probability density function (PDF) curves. The mode of the PDF curves is then selected for the evaluation of the ambient noise level at each station.

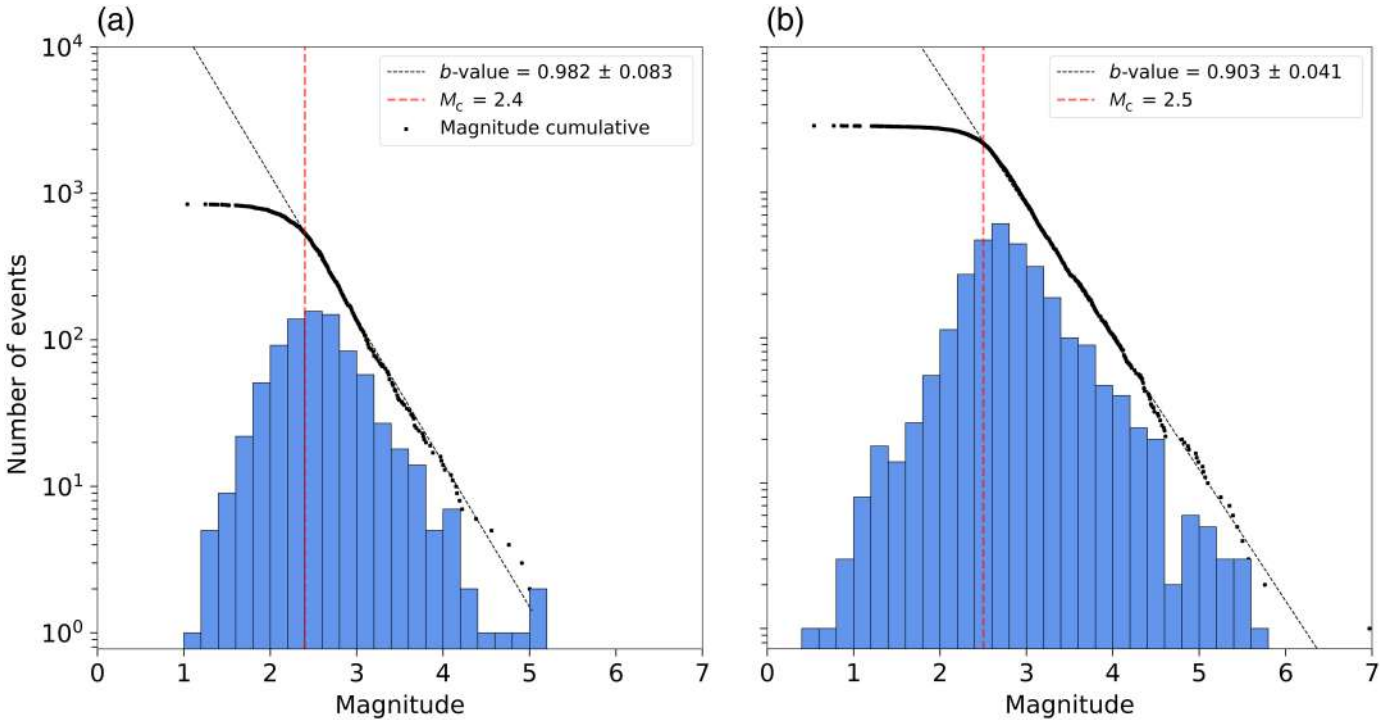

Figure 5. Frequency–magnitude distribution (blue histogram with 0.2 magnitude interval bins) of the Ayiti-Séismes catalog: (a) from August 2019 to 13 August 2021; and (b) from 14 August 2021 to June 2022. M_c indicates magnitude of completeness. The color version of this figure is available only in the electronic edition.

Results

We computed PSD and spectrograms of power values for RS stations of Table 1. The PSD density plot and the mode of the PDF of ten RS stations are presented in Figure S3. For comparison, we also represent in each figure the Peterson (1993) new high- and low-noise models that define the average limits of

TABLE 1
Data Availability of the Ten Stations Used in This Study

	Location		Time Period			
Station Name	**Latitude (°)**	**Longitude (°)**	**From (yyyy/mm/dd)**	**To (yyyy/mm/dd)**	**Data Availability**	**Full Data Availability**
CDELM	18.554	−72.3048	2020/01/20	2020/03/19	96.0%	65.4%
NQBME	18.562	−72.296	2020/01/04	2020/03/31	97.9%	41.9%
SMESL	18.228	−73.616	2021/01/03	2021/03/31	97.6%	93.1%
NPIGN	19.317	−72.127	2020/01/02	2020/02/10	94.1%	49.9%
SJACM	18.236	−72.547	2020/01/15	2020/03/03	73.3%	50.4%
SJER2	18.651	−74.121	2020/01/10	2020/03/31	86.1%	57.5%
CPACO	18.530	−72.327	2020/01/01	2020/03/13	99.9%	83.2%
NHDC1	19.727	−72.233	2020/01/01	2020/02/21	80.8%	60.5%
NMSNI	19.799	−73.383	2020/02/19	2020/03/31	98.0%	50.4%
CGONA	19.456	−72.670	2021/01/14	2021/03/13	93.0%	70.5%

These stations were installed at different time periods since the beginning of the Ayiti-Séismes system from July 2019. The full data availability, since they are operational, varies from 41.9% to 93.1%. Gaps are caused by interruptions in power supply and/or internet connection and defective micro-SD card. For the selected time window between January and March 2020 or 2021 of continuous data sets of each RS station, the availability is >73%. This time window is during the dry season, out of the hurricane season.

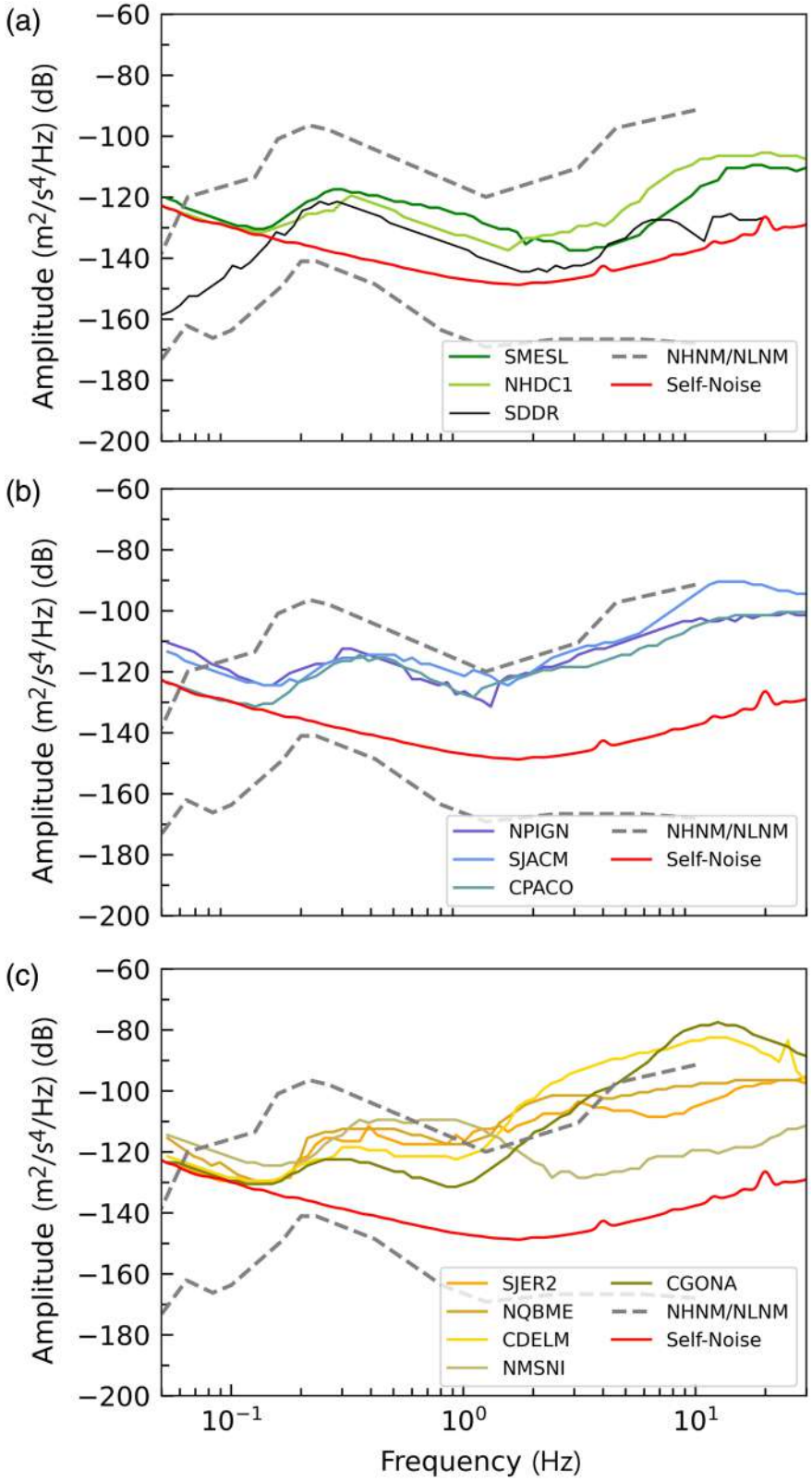

Figure 6. Power density function (PDF) of the ambient-noise level estimates of the RSs' vertical-component geophone using one-, two-, or three-month time window and the methodology of McNamara and Buland (2004). For comparative purposes, we plotted Peterson (1993) new high- and low-noise models (NHNM and NLNM) in gray dashed lines, RS4D geophone self-noise curve as the red line and CU.SDDR BHZ component as the black line. (a) PDF at SMESL RS station (green line)—the quietest of the HY network. (b) PDF of the medium noise stations in this study. (c) PDF of the noisiest stations in this study. The color version of this figure is available only in the electronic edition.

ambient noise obtained from a worldwide network of seismograph stations and RS4D geophone self-noise level used as a benchmark to evaluate our results. This last reference curve is estimated using Sleeman's method (Sleeman, 2006) based on the application of the three-channel correlation technique. This method is based on the precise decomposition of the different noise sources that contribute to the signal measured by the seismic sensors. Using three sensors oriented and positioned at the same site, it is possible to separate and analyze the specific noise contributions of each component of the system. This is a correlation analysis of the recordings from a common and consistent input signal. Using the measurements recorded by each sensor, it is possible to obtain accurate information about the individual characteristics of the self-noise of the entire acquisition chain. For the calculation of this reference presented in Figure S5, we used the vertical component (Z) of three sensors (RS4D, STS-2 v.2, and Trillium Horizon 120) collocated at the Isola station FR.ISO, southeastern France. We also use the BHZ component of the CU.SDDR station's STS-2 sensor as a reference component for noise analysis. We selected four of the stations based on their data availability (93%–99.9%) and also their belonging to the three groups in Figure 6 to implement only the spectrogram of power values method. Between the periods of 0.02 and 1 s the ambient-noise level increases during the day and decreases at night between 02:00 and 09:00 UTC (Fig. S4).

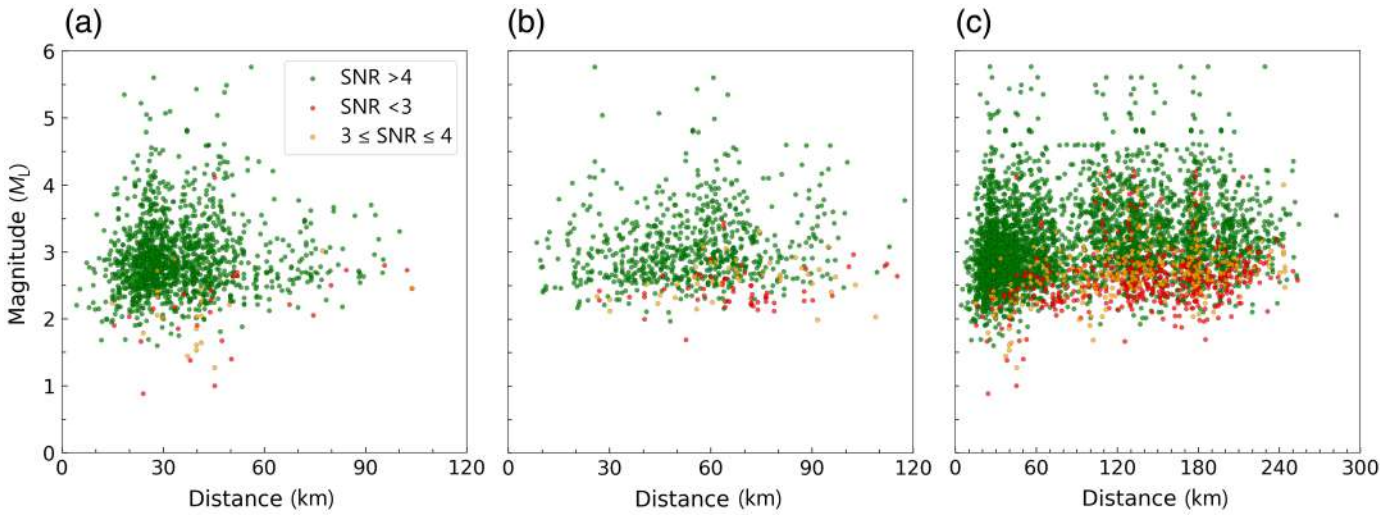

Figure 7. Local magnitude of located earthquakes from July 2020 to January 2022, as a function of epicentral distances for signal-to-noise ratio (SNR ranges). The green background circles are for events with SNR>4 (12 dB), red for SNR<3 (9.5 dB), and orange for 3≤SNR≤4. (a–c) The SNR values, respectively, at RS stations SMESL, SJER2, and at all 10 RS stations studied here. The color version of this figure is available only in the electronic edition.

The mode of the PDF of the ten RS stations are presented in Figure 6, in which they are grouped in three categories. The first one, represented by SMESL and NHDC1 stations (Fig. 6a), has noise levels closest to the SDDR control station noise level between 0.2 and 8.0 Hz. SMESL remains the one that approximates the geophone self-noise mainly between 2 and 10 Hz. The second one (Fig. 6b) includes the stations with higher noise levels that, however, remain below the new high-noise model (NHNM) curve of Peterson (1993). The third one concerns the stations that have the largest PDF mode values (Fig. 6c) that exceed in a frequency range of the new high-noise level curve of Peterson (1993).

At frequencies greater than 0.5 Hz, PDF curves of RS stations are close to or above Peterson's NHNM (Fig. 6b,c). Moreover, because small earthquakes have a frequency content in the 1–20 Hz range, their detection level is affected by this high ambient-noise level and could explain why the magnitude of completeness of Ayiti-Séismes catalog is limited to 2.4–2.5 (Fig. 5). A way to decrease the magnitude of completeness would be to decrease the ambient-noise level at the RS stations, either using an ad hoc installation at the hosts' homes (cellar if available, underground vault, etc.) or by selecting hosts located at places where the anthropogenic noise is measurably low. However, these criteria must be balanced by the fact that RS hosts are volunteers that are limited in numbers. They are usually not willing to modify their personal environment, for example, by drilling, digging, pulling cables, and so forth. Keeping their motivation up—the limited burden of the RS installation is part of it, as shown by Corbet *et al.* (2023)—is essential to the long-term success of our citizen-based initiative.

We illustrate these results using the two stations that recorded the largest number of earthquakes that could be located during the time interval considered here. They are station SMESL, with the lowest noise level in our dataset (Fig. 6a), and the lower quality SJER2 station that belongs to group 3 (Fig. 6c). Figure 7 shows the signal-to-noise ratio (SNR) of their recorded events as a function of hypocentral distance and magnitude. Station SMESL was able to detect earthquakes down to magnitude 1.8 with a high quality (SNR>4) at 20 km distance and magnitude 2.3 at 80 km distance (Fig. 7a). At SJER2 station, the minimum magnitude that permits a high quality is 2.2 at 20 km and 2.5 at 90 km (Fig. 7b).

We then gather the same information for the 10 stations studied here in Figure 7c. We observe that the system was able to detect and locate earthquakes of magnitude at least 2.5 within 200 km of the RS stations, hence covering the entire on-land territory of Haiti and some of its neighboring areas. We also observe that the number of RS stations with an SNR larger than 4 (green dots in Fig. 7c) is not homogeneous with distance, mainly because (1) seismicity was not equally active in all the regions of the country during the time interval studied here; and (2) station distribution is still sparse. In addition, the Ayiti-Séismes detection and location system, as currently parameterized, requires seismic signals from at least four local or regional stations. Of course, even if earthquakes of low magnitude (<1.5 for example) can be detected and located in some areas, the magnitude of completeness of the whole Ayiti-Séismes catalog currently remains at 2.5. Altogether, and considering the low-cost and low-maintenance nature of the RS stations, these are encouraging results, which can only improve, because more RS stations will be installed and because more broadband stations will be restored or installed in Haiti.

Discussion

Seismicity before the M_w 7.2 earthquake of 14 August 2021

The Ayiti-Séismes system detected and located 842 earthquakes, with $M_L \leq 5.0$, from August 2019 to 13 August 2021 (Fig. 3)

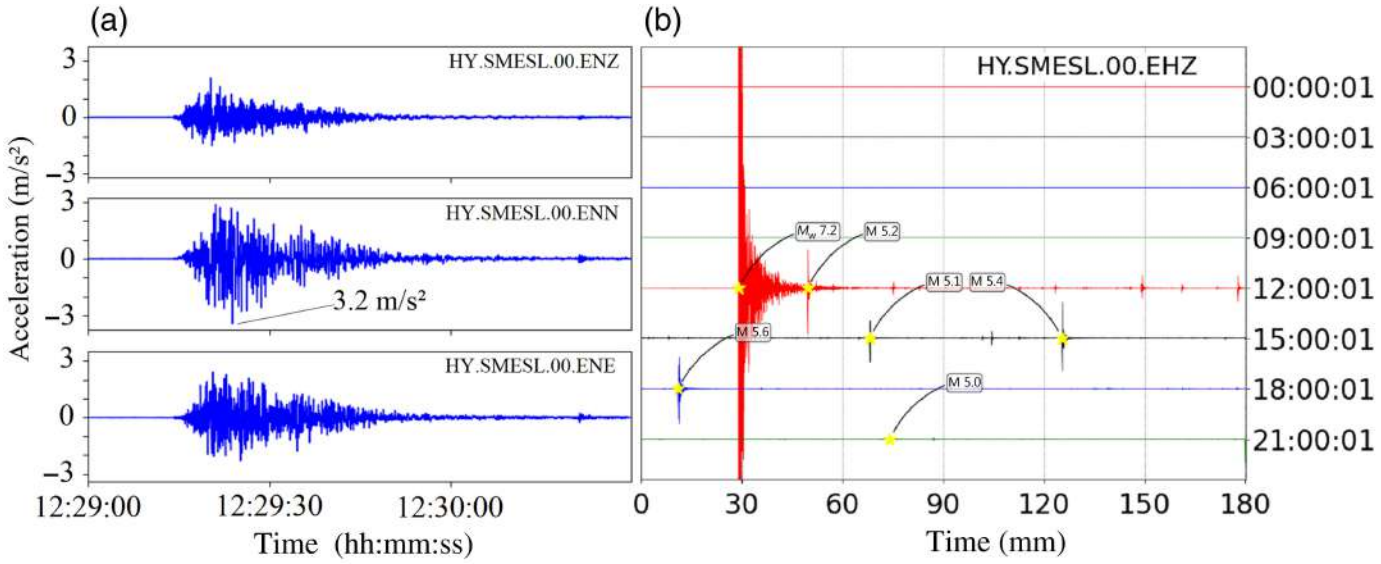

Figure 8. (a) Accelerometric records of the 14 August 2021 M_w 7.2 earthquake at station SMESL on the vertical (ENZ), north–south (ENN), and east–west (ENE) components. Although at a distance of 21 km from the epicenter, none of the three components saturated. (b) Helicorder at station SMESL on 14 August 2010 (vertical velocimeter component) with the main event and five aftershocks of magnitude greater than 5.0. The color version of this figure is available only in the electronic edition.

during a period of interseismic background seismicity. These events are mainly located in the northern and southern parts of the country, broadly distributed on either side of the two major strike-slip plate boundary faults: Enriquillo and Septentrional (Fig. 1). We also observe significant, but diffuse, seismicity scattered between the southern Peninsula and the Gulf of Gonâve, and located offshore for its main part. The central part of the country shows a much lower level of seismicity, with only a few events no larger than M_L 3.0.

In the last decade, two studies analyzed the microseismicity over Haiti. The first one is the analysis of the Dominican Observatorio Sismológico Politécnico Loyola network (Rodriguez *et al.*, 2018) during the 2012–2016 period; events located with the minimum of four stations are poorly located over Haitian territory, but shows a microseismic activity in the southeastern part of the country, which is not present in global catalogs. The second by Possee *et al.* (2019) is the analysis of data from 33 broadband seismometers: 27 from the trans-Haiti temporary network distributed mainly along a north–south profile (Corbeau *et al.*, 2017, 2019) complemented by regional stations. This study covers a period of 16 months in 2013–2014, included in the period analyzed by Rodriguez *et al.* (2018). Event locations are obtained after a travel-time tomography of the area below the seismic network to precise a reliable velocity model and a relocation process. The two main clusters of seismicity are present and were confirmed by template matching analysis (Lee and Douilly, 2023). The first one is concentrated in the epicentral zone of the earthquake of 12 January 2010 along the Enriquillo Plantain Garden fault zone. The second one is at the northeast of Lake Enriquillo, Dominican Republic. But between these two clear clusters one also observes an activity over all the southeastern part of Haiti, which confirms the analysis of Rodriguez *et al.* (2018). The sparse activity observed in the Gulf of Gonâve is not well determined.

Thus, the observations provided by citizen-hosted seismic stations provide new results in the distribution of seismicity in Haiti in spite of the sparse distribution of RS.

RS stations and the Ayiti-Séismes system have allowed for the detection of many more events than previously available, with a spatial completeness much better than what was available with a temporary deployment or with the neighboring seismic network in the Dominican Republic. Therefore, the low level of seismicity recorded in Haiti before seismic stations were in place is a result of the lack of observational capabilities not an actual seismotectonic feature. The ability to significantly decrease the magnitude of completeness (M_c) and improve the geographic detection of earthquakes in Haiti is very important for the future improvements of Haiti and regional seismic hazard maps, because the currently available and official one is based on only 56 **M** > 4 events from the U.S. Geological Survey and International Seismological Centre catalogs (Frankel *et al.*, 2011). One difficulty remains in the fact that a part of relevant seismicity is located offshore, mainly clusters along the Septentrional fault.

The 14 August 2021 M_w 7.2 Nippes earthquake and its aftershocks

The 14 August 2021 M_w 7.2 earthquake and its aftershocks—2712 as of 30 June 2022 in Haiti's southern Peninsula including the 1031 of Calais *et al.* (2022)—were detected and located by the Ayiti-Séismes system. The mainshock was recorded by the least-noisy four-component RS station SMESL (Fig. 8a) at a distance of only 21 km from the rupture. The signal in the seismometer saturated, but the 3D accelerometric sensors were

able to record a ground acceleration of ~0.33*g* on its north–south component (Fig. 8a). This is the first near-field record of strong ground motion in Haiti. During the first day (14 August), the presence of three RS stations in the epicentral area allowed for the detection and location and magnitude determination of 106 aftershocks by the Ayiti-Séismes system. Among them, five had a local magnitude between 5 and 5.6 (Fig. 8b).

This earthquake was a successful test for the RS stations and the Ayiti-Séismes system in several ways. First, it showed that the motivation of the RS citizen hosts is often high, because two of them living in the epicentral area spontaneously found the means to restore their power and Internet connection in the minutes that followed ground shaking. In addition, three additional citizens in the epicentral area volunteered to host an RS; their instruments are still operational as of this writing. Second, it showed that the system (Fig. 2) was able to sustain the data flow and the very large number of detections that followed the mainshock. The resulting, quasi-real-time aftershock locations were then keyed to guide the deployment of field efforts, such as prioritizing the remeasurement of Global Positioning System (GPS) benchmarks and optimizing the location of 12 temporary broadband stations (Douilly *et al.*, 2023). The early aftershock sequence was also used to forecast its evolution—an information that was shared with the local Civil Protection Agency and with relief organizations. Then, the precise relocation of the first month of aftershocks together with complementary space geodetic data allowed us to rapidly and unambiguously determine the rupture mechanism and geometry of this event (Calais *et al.*, 2022).

Contributions of RS instruments to the Haitian context

RS have been increasingly used by many users and network operators since RS 1D personal seismograph launched at Kickstarter's crowdfunding platform on July 2016. However, their experiments have been limited in time to specific case studies. Participatory seismology of the Ayiti-Séismes system is one such study to date, where the viability of these stations over a long period of service has now been tested. The ongoing review of the collective memory of seismic risk in Haiti is progressing with the proactive involvement of citizens in the collection of seismic data—a possibility offered by the simplicity of these small instruments housed in citizens' homes. The choice to place them in a hostile environment, in terms of anthropogenic noise, does not impinge too much in the event detection level and the system's completeness magnitude so that most of the earthquakes felt by the population are also detected by Ayiti-Séismes. One would not expect to detect events with magnitudes below 1 with such an instrument, but the example of the SMESL station shows that improving the density of stations and looking for quieter sites is rather favorable to a decrease of the detection threshold. The ingenuity of the system arouses a certain curiosity among hosts and others, which is perceptible by the increased number of visits per day to the site (from ~70 visits per day before the 14 August 2021 M_w 7.2 Nippes mainshock to ~140 visits per day in June 2022, but with peaks of ~3000 visits per day a few days after the mainshock). The positive impact of this combination reminds people of the existence of seismic risk in Haiti. Many earthquakes, both at sea and on land, are produced in areas not known to be active. These new seismological observations suggest an update of the current seismic hazard map produced in 2010 (Mueller *et al.*, 2015).

Qualitatively, the RS waveforms are globally noisy at high frequency (>1 Hz) by local ambient-noise level. In addition, the stations are installed in very heterogeneous locations that can affect the amplitude of the recorded signals. This would result in a possible contribution to a slight overestimation of local earthquake magnitudes for small events ($M_L < 3$; Anthony *et al.*, 2019). It is possible that events of magnitude less than 2 are absorbed in the intrinsic noise of the instrument, thus undetectable at large distances. This impacts the existing threshold with respect to location criteria. In this context, any event detected is not necessarily locatable and therefore not cataloged.

Implicitly, seismic monitoring implies the search for new tectonically active structures, if they exist. This should be satisfied by the densification of the HY network, given the first results obtained with the RS stations deployed near the epicentral zone of the 14 August 2021 M_w 7.2 earthquake. There is also a strong interest for nearby networks, such as the Cuban and Dominican seismic networks, to include in their own processing HY real-time dataflow to better determine seismicity at their borders.

Conclusion

We examined the variation of ambient noise level of a sample of 10 RS by the PSD method and used the Gutenberg–Richter law to establish the detection threshold of the Ayiti-Séismes system. Our results show that combining low-cost stations with conventional stations provides scientifically relevant information for real-time monitoring of seismicity in Haiti. The exploitation of this information shows that RS stations have the potential to be used for earthquake monitoring in countries where conventional seismic networks are difficult to maintain.

The Ayiti-Séismes system, operational since August 2019, has recorded more than 4000 earthquakes, obtained an unsaturated record of the M_w 7.2 earthquake of August 2021, and detected hundreds of its aftershocks. In spite of the high level of noise at most RS stations, the magnitude of completeness of the network is 2.5, which makes it possible to detect and locate felt earthquakes, and thus provide quasi-real-time information to rapidly inform the population and the authorities. This completeness magnitude, together with the spatial and temporal distribution of the seismicity allowed by RS instruments and

the Ayiti-Séismes system, provides a significantly improved earthquake catalog for Haiti compared to those obtained from far-field regional seismic stations or temporary seismic deployments. In addition to contributing to the general understanding of the country's and the plate boundary's seismotectonics, this catalog has the potential to significantly contribute to the next generation of regional seismic hazard maps.

To improve the system, we are planning to significantly increase the number of RS stations throughout Haiti, with regional redundancy in some cases to mitigate the issues related to access to the electricity or to the Internet. Because this deployment is part of an interdisciplinary project (toward a multi-stakeholder socio-seismological observation network for seismic risk reduction in Haiti) that involves both seismologist and social scientists, we seek to diversify the social demographics of the hosts as much as to improve site characteristics. Because one of the main problems is the power supply and the availability of the internet network, it is planned that some stations will be located in more viable places, like, for example, school establishment's partners of the project. Machine learning techniques are under development to optimize the use of noisy signals at the RS stations. Ultimately, this approach aims at complementing reliable broadband stations, which should still provide the robust backbone for earthquake detection and other seismological applications.

Data and Resources

The seismic data and metadata used in this article are accessible from the Ayiti-Séismes system available at ayiti.unice.fr/ayiti-seismes/. Data network code is HY available at 10.7914/sn/hy. All the data and metadata are freely available at the Institutions of Research in Seismology (IRIS) and from the webservices of the International Federation of Digital Seismograph Networks (FDSN). METEOR is an online tool available at https://meteor.unice.fr. SyNApSE is an online tool that monitors and retrieves health data from remote stations, sends notifications, and displays metric values. This system lets operators track station health, store supervision values, and diagnose failures. A presentation of SyNApSE can be available at https://www.resif.fr/donnees-et-produits/logiciels-et-outils/. SyNApSE, Gaaaaaps (https://ayiti.unice.fr/gaaaaaps/), and Webpicker are tools available internally at Géoazur Laboratory. The seismic datasets were processed using standard processing steps, taking advantage of the ObsPy package (Beyreuther *et al.*, 2010) for Python. Map of station and earthquake locations are made with the Generic Mapping Tools (GMT; Wessel *et al.*, 2013). All websites were last accessed August 2023. The supplemental material includes two examples of the installation of Raspberry Shake (RS) stations in Haiti, data from the RS stations studied available between July 2019 and 30 June 2022, probability density function (PDF), spectrogram of power spectral density (PSD), and self-noise curves of the vertical component of three seismometers are provided in addition.

Declaration of Competing Interests

The authors acknowledge that there are no conflicts of interest recorded.

Acknowledgments

The authors deeply thank the individuals and organizations that are currently hosting Raspberry Shake (RS) stations in Haiti; they make a difference! The authors acknowledge the persons in charge of seismic data from regional networks in the Dominican Republic, Cuba, Jamaica, Canada, Puerto Rico, and United States, and thank their operating agencies for making them available. The authors thank Christophe Maron for his help in building instrumental responses. This work was supported by the Centre National de la Recherche Scientifique (CNRS) and the Institut de Recherche pour le Développement (IRD) through their "Natural Hazard" program ("S2RHAI" project); the FEDER European Community program within the Interreg Caraïbes "PREST" project; Université Côte d'Azur and the French Embassy in Haiti win support of SP's PhD; the French National Research Agency (project ANR-21CE03-0010 "OSMOSE").

Author contributions: The Ayiti-Séismes system was developed by Jérôme Chèze and Fabrice Peix. The daily verification and relocation of earthquakes has been performed by Tony Monfret, Anne Deschamps, Francoise Courboulex, and Sylvert Paul. The installation and maintenance of the RS stations are driven by Steeve Julien Symithe and Eric Calais. The preparation of the article and figures was done by Sylvert Paul, Anne Deschamps, Tony Monfret, Francoise Courboulex, Eric Calais, David Ambrois, and Jérôme Chèze. All authors discussed the results, and contributed to the final article.

References

Aki, K. (1965). Maximum likelihood estimate of b in the formula log N= a-bM and its confidence limits, *Bull. Earthq. Res. Inst.* **43,** 237–239.

Anthony, R. E., A. T. Ringler, D. C. Wilson, and E. Wolin (2019). Do low-cost seismographs perform well enough for your network? An overview of laboratory tests and field observations of the OSOP raspberry shake 4D, *Seismol. Res. Lett.* **90,** no. 1, 219–228, doi: 10.1785/0220180251.

Bakun, W. H., C. H. Flores, and U. S. ten Brink (2012). Significant earthquakes on the Enriquillo Fault System, Hispaniola, 1500-2010: Implications for seismic hazard, *Bull. Seismol. Soc. Am.* **102,** no. 1, 18–30, doi: 10.1785/0120110077.

Bent, A. L., J. Cassidy, C. Prépetit, M. Lamontagne, and S. Ulysse (2018). Real-time seismic monitoring in Haiti and some applications, *Seismol. Res. Lett.* **89,** no. 2A, 407–415, doi: 10.1785/0220170176.

Beyreuther, M., R. Barsch, L. Krischer, T. Megies, Y. Behr, and J. Wassermann (2010). ObsPy: A python toolbox for seismology, *Seismol. Res. Lett.* **81,** no. 3, 530–533, doi: 10.1785/gssrl.81.3.530.

Calais, E., D. Boisson, S. Symithe, C. Prépetit, B. Pierre, S. Ulyse, L. Hurbon, A. Gilles, J.-M. Théodat, T. Monfret, *et al.* (2020). A socio-seismology experiment in Haiti, *Front. Earth Sci.* **8,** 542,654, doi: 10.3389/feart.2020.542654.

Calais, E., A. Freed, G. Mattioli, F. Amelung, S. Jónsson, P. Jansma, S.-H. Hong, T. Dixon, C. Prépetit, and R. Momplaisir (2010). Transpressional rupture of an unmapped fault during the 2010 Haiti earthquake, *Nature Geosci.* **3,** no. 11, 794–799, doi: 10.1038/ngeo992.

Calais, E., S. Symithe, T. Monfret, B. Delouis, A. Lomax, F. Courboulex, J. P. Ampuero, P. E. Lara, Q. Bletery, J. Chèze, F. Peix, *et al.* (2022). Citizen seismology helps decipher the 2021 Haiti earthquake, *Science* **376,** no. 6590, 283–287, doi: 10.1126/science.abn1045.

Chèze, J., C. Maron, D. Rivet, F. Peix, D. Brunel, X. Martin, and B. Delouis (2020). METEOR: Online seismic metadata builder, *Seismol. Res. Lett.* **92,** no. 2A, 1141–1147, doi: 10.1785/0220200217.

Cooley, J. W., and J. W. Tukey (1965). An algorithm for the machine calculation of complex Fourier series, *Math. Comput.* **19,** no. 90, 297–301, doi: 10.2307/2003354.

Corbeau, J., O. L. Gonzalez, V. Clouard, F. Rolandone, S. Leroy, D. Keir, G. Stuart, R. Momplaisir, D. Boisson, and C. Prépetit (2019). Is the local seismicity in western Hispaniola (Haiti) capable of imaging northern Caribbean subduction? *Geosphere* **15,** no. 6, 1738–1750.

Corbeau, J., F. Rolandone, S. Leroy, K. Guerrier, D. Keir, G. Stuart, V. Clouard, R. Gallacher, S. Ulysse, D. Boisson, *et al.* (2017). Crustal structure of western Hispaniola (Haiti) from a teleseismic receiver function study, *Tectonophysics* **709,** 9–19, doi: 10.1016/j.tecto.2017.04.029.

Corbet, A., L. Fallou, N. Calixte, L. Hurbon, and E. Calais (2023). From a seismological network to a socio- seismological one: A citizen science experiment in Haïti to reduce seismic risk: Analysis of a "Small Box" that can do a lot, *Citizen Sci.* **8,** no. 1, 2, doi: 10.5334/cstp.481.

DeMets, C., P. E. Jansma, G. S. Mattioli, T. H. Dixon, F. Farina, R. Bilham, E. Calais, and P. Mann (2000). GPS geodetic constraints on Caribbean-North America plate motion, *Geophys. Res. Lett.* **27,** no. 3, 437–440, doi: 10.1029/1999GL005436.

Diaz, J., M. Schimmel, M. Ruiz, and R. Carbonell (2020). Seismometers within cities: A tool to connect earth sciences and society, *Front. Earth Sci.* **8,** 9, doi: 10.3389/feart.2020.00009.

Douilly, R., S. Paul, T. Monfret, A. Deschamps, D. Ambrois, S. J. Symithe, S. St Fleur, F. Courboulex, E. Calais, D. Boisson, *et al.* (2023). Rupture segmentation of the 14 August 2021 Mw 7.2 Nippes, Haiti, earthquake using aftershock relocation from a local seismic deployment, *Bull. Seismol. Soc. Am.* **113,** no. 1, 58–72, doi: 10.1785/0120220128.

Fallou, L., A. Corbet, N. Calixte, L. Hurbon, E. Calais, J.-M. Theodat, F. Courboulex, R. Bossu, K. Guerrier, G. Etienne, *et al.* (2022). Building an efficient and inclusive communication strategy for risk reduction in Haiti through a citizen-seismology approach, *No. EGU22-9942. EGU22, Copernicus Meetings*, Vienna, Austria, 23–27 May 2022, doi: 10.5194/egusphere-egu22-9942.

Frankel, A., S. Harmsen, C. Mueller, E. Calais, and J. Haase (2011). Seismic hazard maps for Haiti, *Earthq. Spectra* **27,** no. 1_suppl1, 23–41, doi: 10.1193/1.3631016.

Gailler, A., E. Calais, H. Hebert, C. Roy, and E. Okal (2015). Tsunami scenarios and hazard assessment along the northern coast of Haiti, *Geophys. J. Int.* **203,** no. 3, 2287–2302, doi: 10.1093/gji/ggv428.

Gulia, L., A. P. Rinaldi, T. Tormann, G. Vannucci, B. Enescu, and S. Wiemer (2018). The effect of a mainshock on the size distribution of the aftershocks, *Geophys. Res. Lett.* **45,** no. 24, doi: 10.1029/2018GL080619.

Hayes, G. P., R. W. Briggs, A. Sladen, E. J. Fielding, C. Prentice, K. Hudnut, P. Mann, F. W. Taylor, A. J. Crone, R. Gold, *et al.* (2010). Complex rupture during the 12 January 2010 Haiti earthquake, *Nat. Geosci.* **3,** no. 11, 800–805, doi: 10.1038/ngeo977.

Helmholtz-Centre Potsdam-GeoForschungsZentrum (GFZ) German Research Centre For Geosciences and Global Earthquake Monitoring Processing Analysis (GEMPA) GmbH (2008). The SeisComP seismological software package, *GFZ Data Services*, doi: 10.5880/GFZ.2.4.2020.003.

Holmgren, J. M., and M. J. Werner (2021). Raspberry shake instruments provide initial ground-motion assessment of the induced seismicity at the united downs deep geothermal power project in Cornwall, United Kingdom, *Seismic Records* **1,** no. 1, 27–34, doi: 10.1785/0320210010.

Hough, S. E., S. S. Martin, S. J. Symithe, and R. Briggs (2023). Rupture scenarios for the 3 June 1770 Haiti earthquake, *Bull. Seismol. Soc. Am.* **113,** no. 1, 157–185, doi: 10.1785/0120220108.

Jeddi, Z., P. H. Voss, M. B. Sørensen, F. Danielsen, T. Dahl-Jensen, T. B. Larsen, G. Nielsen, A. Hansen, P. Jakobsen, and P. O. Frederiksen (2020). Citizen seismology in the arctic, *Front. Earth Sci.* **8,** 139, doi: 10.3389/feart.2020.00139.

Johnson, K., M. Pagani, and T. Chartier (2021). *Probabilistic Seismic Hazard Model for the Dominican Republic, D.2.2.2, v2.0.0, October 2021*, Global Earthquake Model Foundation, Italy.

Lamb, O. D., M. J. Shore, J. M. Lees, S. J. Lee, and S. M. Hensman (2021). Assessing raspberry shake and boom sensors for recording African elephant acoustic vocalizations, *Front. Conserv. Sci.* **1,** 630,967, doi: 10.3389/fcosc.2020.630967.

Lecocq, T., S. P. Hicks, K. Van Noten, K. van Wijk, P. Koelemeijer, R. S. M. De Plaen, F. Massin, G. Hillers, R. E. Anthony, M.-T. Apoloner, *et al.* (2020). Global quieting of high-frequency seismic noise due to COVID-19 pandemic lockdown measures, *Science* **369,** no. 6509, 1338–1343, doi: 10.1126/science.abd2438.

Lee, H. Y., and R. Douilly (2023). Earthquake swarms in southern Hispaniola revealed by spatiotemporal evolution of seismicity from multi-station template matching, *Bull. Seismol. Soc. Am.* **113,** no. 1, 115–130, doi: 10.1785/0120220125.

Manaker, D. M., E. Calais, A. M. Freed, S. T. Ali, P. Przybylski, G. Mattioli, P. Jansma, C. Prépetit, and J. B. Chabalierde (2008). Interseismic plate coupling and strain partitioning in the northeastern Caribbean, *Geophys. J. Int.* **174,** no. 3, 889–903, doi: 10.1111/j.1365-246X.2008.03819.x.

Manconi, A., V. Coviello, M. Galletti, and R. Seifert (2018). Short communication: Monitoring rockfalls with the Raspberry Shake, *Earth Surf. Dynam.* **6,** no. 4, 1219–1227, doi: 10.5194/esurf-6-1219-2018.

Mann, P., F. W. Taylor, R. L. Edwards, and T.-L. Ku (1995). Actively evolving microplate formation by oblique collision and sideways motion along strike-slip faults: An example from the northeastern Caribbean plate margin, *Tectonophysics* **246,** nos. 1–3, 1–69, doi: 10.1016/0040-1951(94)00268-E.

Martin, S. S., and S. E. Hough (2022). The 8 April 1860 Jour de Pâques earthquake sequence in southern Haiti, *Bull. Seismol. Soc. Am.* **112,** no. 5, 2468–2486, doi: 10.1785/0120220016.

McCann, W. R. (2006). Estimating the threat of tsunamigenic earthquakes and earthquake induced-landslide tsunami in the Caribbean, *Caribbean Tsunami Hazard* 43–65, doi: 10.1142/9789812774613_0002.

McNamara, D. E., and R. P. Buland (2004). Ambient noise levels in the continental United States, *Bull. Seismol. Soc. Am.* **94,** no. 4, 1517–1527, doi: 10.1785/012003001.

Moreno Toiran, B. (2002). The new Cuban seismograph network, *Seismol. Res. Lett.* **73,** no. 4, 504–517, doi: 10.1785/gssrl.73.4.504.

Mueller, C. S., R. W. Briggs, R. L. Wesson, and M. D. Petersen (2015). Updating the USGS seismic hazard maps for Alaska, *Quat. Sci. Rev.* **113,** 39–47, doi: 10.1016/j.quascirev.2014.10.006.

Peterson, J. R. (1993). *Observations and Modeling of Seismic Background Noise, Open-File Rept. No. 93–322*, U.S. Geological Survey, Albuquerque, New Mexico, U.S.A., doi: 10.3133/ofr93322.

Possee, D., D. Keir, N. Harmon, C. Rychert, F. Rolandone, S. Leroy, J. Corbeau, G. Stuart, E. Calais, F. Illsley-Kemp, *et al.* (2019). The tectonics and active faulting of Haiti from seismicity and tomography, *Tectonics* **38,** no. 3, 1138–1155, doi: 10.1029/2018TC005364.

re3data.org (2022). Résif seismological data portal, editing status 2 February 2023; re3data.org—Registry of Research Data Repositories, doi: 10.17616/R37Q06.

Rodriguez, J., J. Havskov, M. B. Sørensen, and L. F. Santos (2018). Seismotectonics of south-west Dominican Republic using recent data, *J. Seismol.* **22,** no. 4, 883–896, doi: 10.1007/s10950-018-9738-9.

Scherer, J. (1912). Great earthquakes in the Island of Haiti, *Bull. Seismol. Soc. Am.* **2,** no. 3, 161–180.

Shelly, D. R., G. C. Beroza, and S. Ide (2007). Non-volcanic tremor and low-frequency earthquake swarms, *Nature* **446,** no. 7133, 305–307.

Sleeman, R. (2006). Three-channel correlation analysis: a new technique to measure instrumental noise of digitizers and seismic sensors, *Bull. Seismol. Soc. Am.* **96,** no. 1, 258–271, doi: 10.1785/0120050032.

Subedi, S., G. Hetényi, P. Denton, and A. Sauron (2020). Seismology at school in Nepal: A program for educational and citizen seismology through a low-cost seismic network, *Front. Earth Sci.* **8,** 73, doi: 10.3389/feart.2020.00073.

Symithe, S., E. Calais, J. B. de Chabalier, R. Robertson, and M. Higgins (2015). Current block motions and strain accumulation on active faults in the Caribbean: Current Caribbean kinematics, *J. Geophys. Res.* **120,** no. 5, 3748–3774, doi: 10.1002/2014JB011779.

SyNApSE (2021). le Système National pour la Supervision des Équipements, *Lettre du RAP, RESIF*, N°32, available at https://rap.resif.fr/wp-content/uploads/sites/5/2022/03/lettrerap_32_2021_semestre1.pdf (last accessed August 2023) (in French).

Taruselli, M., D. Arosio, L. Longoni, M. Papini, and L. Zanzi (2019). Raspberry shake sensor field tests for unstable rock monitoring, *1st Conference on Geophysics for Infrastructure Planning Monitoring and BIM*, European Association of Geoscientists and Engineers, The Hague, Netherlands, Vol. 2019, 1–5, doi: 10.3997/2214-4609.201902558.

ten Brink, U. S., W. H. Bakun, and C. H. Flores (2011). Historical perspective on seismic hazard to Hispaniola and the northeast Caribbean region, *J. Geophys. Res.* **116,** no. B12, 10.1029/2011JB008497.

Université d'Etat d'Haiti (2019). UEH seismic network [Data set], *International Federation of Digital Seismograph Networks*, doi: 10.7914/SN/HY.

Utrera, C. D. (1927). Santo domingo: Dilucidaciones históricas, *Imprenta de Dios y Patria*, available at http://bibliotecadigital.bnphu.gob.do:8080/handle/BNPHU/254 (last accessed August 2023) (in Spanish).

Wessel, P., W. H. F. Smith, R. Scharroo, J. Luis, and F. Wobbe (2013). Generic mapping tools: Improved version released, *Eos Trans. AGU* **94,** no. 45, 409–410, doi: 10.1002/2013EO450001.

Wiggins-Grandison, M. (2001). Preliminary results from the new Jamaica seismograph network, *Seismol. Res. Lett.* **72,** no. 5, 525–537.

Winter, K., D. Lombardi, A. Diaz-Moreno, and R. Bainbridge (2021). Monitoring icequakes in east Antarctica with the Raspberry Shake, *Seismol. Res. Lett.* doi: 10.1785/0220200483.

Zhou, Y., H. Yue, L. Fang, S. Zhou, L. Zhao, and A. Ghosh (2022). An earthquake detection and location architecture for continuous seismograms: Phase picking, association, location, and matched filter (PALM), *Seismol. Res. Lett.* **93,** no. 1, 413–425.

Zhu, W., and G. C. Beroza (2019). PhaseNet: A deep-neural-network-based seismic arrival-time picking method, *Geophys. J. Int.* **216,** no. 1, 261–273.

Manuscript received 24 February 2023
Published online 6 September 2023